International Society for Rock Mechanics and Rock Engineering
Norwegian Group for Rock Mechanics

ISRM International Symposium
Eurock 2025 – Expanding the Underground Space
Trondheim, Norway, 16-20 June
ISBN 978-82-8208-079-8

Specimen Height-to-Diameter Ratio Effect on Failure Modes of Tall Pillars

F. T. Suorineni
Nazarbayev University, Astana, Kazakhstan
fidelis.suorineni@nu.edu.kz (email of corresponding author)

Y. Madenova
Los Alamos National Laboratory, Los Alamos, NM, USA

N. Baizhiyen
University of Adelaide, Adelaide, South Australia, Australia

Abstract

The performance of underground excavations and pillars is a function of the excavation geometry, stress, and host rock mechanical properties. Design of conventional underground mine pillars considers the pillar width to height ratio (W/H) that ranges from 1 to 4 and translates to H/W ratio of 0.25 to 1. There is a volume of work in the literature on specimen H/D ratio and specimen geometry effect on rock strength, failure modes and mechanisms. Existing research largely addresses specimen H/D ratios up to 3, leaving a gap in the understanding of tall pillars. This study investigates the concept of unconventional tall pillars and underground excavations, where pillar or column H/D ratio is equal to or greater than 6. Finite element numerical modeling and laboratory experiments were used to test this concept and examine the failure mechanism of the unconventional underground tall pillars. A total of 35 uniaxial compressive strength tests on rock core samples with H/D ratios of 2 to 8 were conducted. The results reveal that specimens with H/D ratios of 6 or higher primarily fail through bending-induced tension, contrasting with shorter specimens, which fail by tensile splitting, shear, or crushing, as often seen in ISRM and ASTM standard tests. The failure characteristics of these specimens suggest that the tensile strength instead of the uniaxial compressive strength should be used for design of tall pillars, columns, or beams with H/D ratios equal to or greater than 6. The application of the slenderness ratio for designing tall pillars is also explored but requires further research.

Keywords

Height to diameter ratio, tall pillars, failure mechanism, buckling, tensile strength

ISRM

NBG

1 Introduction

Underground structures dimensions are important parameters in underground excavation design that affects rock strength, failure modes and mechanisms. Substantial research has been conducted on specimen height to diameter (H/D) ratio effect including those of Vogler and Stacey (2016), and Masoumi et al. (2012, 2015, 2018). Vogler and Stacey tested a limited number of core specimens of different H/D ratios and concluded that specimen H/D ratio influence the stress-strain curve in the post peak region where the test results gave different slopes, implying that these slopes are not material constants as they are specimen geometry dependent. Masoumi et al. (2012, 2015, 2018) investigated the effect of core H/D ratios on rock strength using both point load strength and uniaxial compressive strength (UCS) tests on various rock types. These authors concluded that the Hoek and Brown (1980) size effect relationship does not apply to their tested rocks and that the size effect also depended on test method. Kong et al. (2021) conducted a comprehensive review of research on size effect including their own test work and arrived at similar conclusions to those of Masoumi et al. and Hawkins (1998). In general, most of the work on specimen H/D ratio or geometric effects are limited to ratios of 0.08 to 3 and the UCS often decreases from small diameter specimens to a nearly constant value with increase in specimen diameter. This paper investigates the failure modes of specimens with various H/D ratios and discusses the implications of buckling failure mechanism for underground excavation design. Particularly, the emphasis is on the design of structurally controlled underground excavation walls and hard rock mine pillars.

2 Failure Modes of Underground Pillars and Excavations

2.1 Hard rock pillar failure modes

A pillar fails when its compressive load exceeds its peak strength. Study shows that pillar stability is mostly dependent on the pillar geometry (width to height ratio) rather than its intact rock UCS (Mark and Barton 1996). Table 1 provides a classification of pillars based on size and shape using pillar width to height (W/H) ratio. The pillar width to height ratio is redefined as H/W in line with specimen geometry descriptions in accordance with both ASTM and ISRM standards for rock strength (uniaxial and triaxial compression tests) determination purposes.

Table 1 Classification of pillars based on size and shape

Ratio of pillar dimension	Squat pillars	Intermediate pillars	Slender pillars	Tall pillars
W/H	≥ 2.5	1.0 to 2.5	0.2 to 1.0	≤ 0.17
H/W	≥ 0.4	0.4 to 1.0	1 to 5	≥ 6.0

Squat pillars have high load bearing capacity due to confinement effect around the pillar core. In standard squat pillars, the failure process commences at the pillar corners as spalling, sloughing, and fracturing and propagates towards the pillar center (Krauland and Soder 1987; Lunder 1994). For intermediate pillars failure is often in the form of simple shearing, conical failure (two intersection shear planes) or axial splitting. Slender pillars fail by crushing or tensile splitting as noted by Esterhuizen (2006). The failure of slender pillars could be in a violent and sudden manner shedding the entire load and causing massive collapse (domino pillar failure).

Table 1 introduces pillar classification with the definition of a tall pillar geometry, which is the focus of this study. The concept of tall pillars is based on the hypothesis that when a structural unit such as a pillar has its height far greater than its width or diameter its failure will not be governed by the intact rock uniaxial compressive strength but rather by buckling and tensile strength. In this study, it is hypothesized that after a certain H/W ratio, slender pillars will fail in tension by bending rather than by tensile splitting. Numerical modeling and laboratory experiments are used to test this hypothesis and to identify the specimen height to diameter (H/D) ratio beyond which specimens fail in tension by buckling or bending.

2.2 Failure modes in underground excavations

Underground excavations walls in some rockmasses can be seen as consisting of several columns in excavations walls and of beams in excavation roofs and floors particularly in foliated rockmasses and in rocks with vertical discontinuities. These columns and beams can be considered as tall pillars. A common mode of failure in such excavations walls and roofs is buckling as shown in Fig. 1. Sharrock and Chapula (2020) describe the host rock mass in Fig. 1a as comprising predominantly thinly bedded siltstone steeply dipping west (80°). The host rock mass also has a northerly trending axial planar cleavage that dips steeply east (80°). At the site described the accepted major principal stress direction is approximately east-west. According to Sharrock and Chapula (2020), the sidewalls of tunnels driven near-parallel to bedding (e.g., perimeter drives, and ore-zone strike drives) are prone to much higher levels of buckling damage (Fig. 1a) than those driven perpendicular to bedding (such as crosscuts). Note that the bulking seen in Fig. 1a is not due to rockbursting.

Several authors, including Cai and Kaiser (2018), Jia and Tang (2008), Karampinos et al. (2015), Masoudi and Sharifzadeh (2018), Jin et al. (2018), and Hu et al. (2021) have written extensively on buckling failure of excavation sidewalls. In most of these cases the buckling is described as squeezing. A unique characteristic of the buckling failures in excavation walls is that the rockmass have sub-vertical or sub-horizontal discontinuities in the excavation walls in the form of columns (excavation walls) or beams in the excavation roofs as shown in Fig. 1b and 1c. In Fig.1b, it is obvious that the height of the sidewall columns (excavation height) is far greater than the width of the columns and falls into the category of tall pillars in Table 1.

(a) (b) (c)

Fig. 1 Buckling failure of (a) excavation side walls in a rockmass with sub-vertical discontinuity sets (Sharrock and Chapula 2020); (b) excavation wall (Hu et al. 2021); (c) excavation floor (Zhou et al. 2024).

3 Proof of Concept

3.1 Numerical modelling

Numerical modelling was conducted first to explore the validity of the research hypothesis. In this study, RS2 (RocScience 2019), a two-dimensional (2D) finite element software, was used for numerical modelling. As the main objective of this research is to determine the H/D ratio beyond which slender pillars must be defined as tall pillars, numerical models were constructed for various H/D ratios ranging from 2 to 8 for a total of seven models. The input parameters and boundary conditions for all models were kept unchanged. Each model was fixed at the bottom. Uniform continuous loading was applied in compression at the top, and the model was allowed to deform vertically and laterally. The input parameters of the models were determined in the laboratory using standard laboratory tests as described in Ulusay (2015), and they are provided in Table 2. Five specimens were tested according to the ISRM standards, and the mean value was taken.

Table 2 Average input parameters determined in the laboratory and used in the models

Rock type	UCS, σ_c (MPa)	Elastic Modulus, E (GPa)	Poisson's ratio, ν	Frictional angle, ϕ^o	Cohesion, c (MPa)
Quartz microquartzite	68.7	13.46	0.27	48.4	3.6

The modelling results based on plastic analysis are shown in Fig. 2. The choice of plastic rather than elastic modeling was to enable observation of the deformed shapes of the different H/D ratios models. Figure 2 demonstrates that models with H/D ratios less than or equal to 5 deformed by barreling, while specimens with H/D ratios equal to or greater than 6 tended to bend (buckle) by deflection from the vertical, with the bending becoming more conspicuous at higher H/D ratios. This implies that rock cores bending under compressive loads will fail in tension, starting from the outer fiber, as suggested in the research hypothesis. These results suggest that slender pillars become tall pillars when their height to width ratio is equal to or greater than 6. Specimens with H/D ratio less than 6 behave like the standard specimens with H/D ratio between 2.5-3 as recommended by ISRM (Ulusay 2015) for standard compression tests.

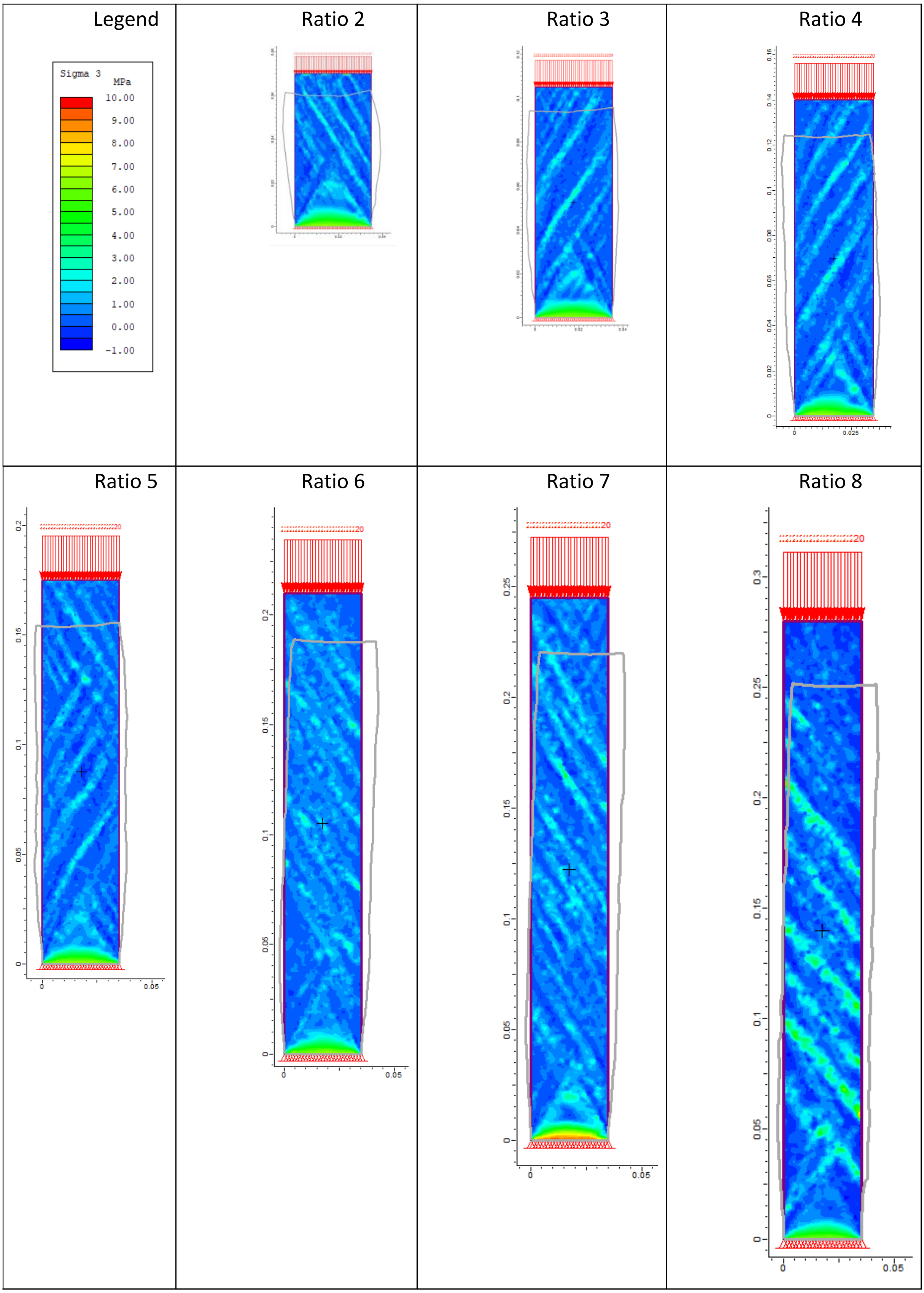

Fig. 2 Results of the numerical modelling of seven specimens with various H/D ratios for proof of tall pillar concept and for determination of the minimum H/D ratio at which slender pillars are classified as tall pillars (Baizhiyen 2019).

3.2 Laboratory testing – validation of the numerical modelling results

Based on the numerical modelling results, laboratory tests were conducted on 35 rock core specimens with the diameter of 35-mm and with H/D ratios ranging from 2 to 8. These core specimens were collected from Ridder-Sokolny Mine in East Kazakhstan and are described as quartz-sericite-microquartzites. Specimen preparation, testing, and UCS calculation procedures followed the ISRM suggested standard (Ulusay 2015) except for the specimen H/D ratios, which had to be varied to achieve the research objectives. Determination of intact rock UCS according to the ISRM standard requires specimens with diameter of 50 mm and H/D ratio between 2.5 and 3.0 (Ulusay 2015). To address this requirement, UCS values from the 35mm-diameter specimens were corrected to 50 mm-diameter size specimens using Eq. (1) proposed by Hoek et al. (1995).

$$\frac{\sigma_{c50}}{\sigma_c} = \left[\frac{D}{50}\right]^{0.18} \tag{1}$$

Where σ_{50} UCS of a 50 mm diameter specimen
σ_c UCS of the tested specimen
D Diameter of the tested specimen

The laboratory rock tests were supplemented with uniaxial compression and indirect tensile strength (ITS) testing of concrete specimens made from a mixture of sand and cement and cast according to ASTM standards. The concrete specimens had a diameter of 37 mm and H/D ratio of 2, 4, 5, 6, 7 and 8 like the rock core specimens. In all, thirty-eight concrete specimens were tested at various H/D ratios in uniaxial compression, and 20 in the indirect tensile strength testing (ITS) or Brazilian tensile strength tests. For the purposes of space, only the rock test results are reported in this paper since the results for the concrete specimens are like those of the rocks.

Figure 3(a)-(d) shows the failed rock cores with H/D ratios of 2, 3, 4 and 5 under UCS tests. As can be seen, these specimens failed by axial splitting, shearing along discontinuities, and crushing. These modes of failure are like those reported by Basu et al. (2013) and expected as per ISRM and ASTM standard UCS testing. In contrast, Figure 3(e)-(g) shows that specimens with H/D ratio of 6, 7 and 8 mostly failed by sharp breaks across the specimen diameter at some point along the height. This failure mode is characteristic for the samples with H/D≥6. According to observations of Esterhuizen (2006), brittle failure in slender pillars can commence near the pillar center, which is proven by laboratory evidence in this study. The mechanism of induced failure of rock specimens with H/D greater than 5 is identical to the failure process in the direct tensile strength test in which specimens are subjected to axial tensile loading and fail in tension. Thus, it can be stated that tall specimens with H/D≥6 fail in tension by bending as in Fig. 3(e) to (g) and demonstrated in Fig. 4a.

(a) Failure modes of rock specimens with H/D ratio of 2

(b) Failure modes of rock specimens with H/D ratio of 3

(c) Failure modes of specimens with H/D ratio of 4

(d) Failure modes of specimens with H/D ratio of 5

(e) Failure modes of specimens with H/D ratio of 6

(f) Failure modes of specimens with H/D ratio of 7

(g) Failure modes of specimens with H/D ratio of 8

Fig. 3 Failure modes of rock specimens with various H/D ratio under UCS. Specimens with H/D ratios of <6 failed by shearing, tensile splitting or crushing (a) to (e), Specimen with H/D≥6 failed in tension by bending ((e) to (g)) and can be classified as tall pillars.

4. Discussion

The results of this study suggest that in dealing with core specimens or underground mine pillars of different height to diameter ratios it may be more appropriate to use the slenderness ratio (Fig. 4b) as in Popov (1978), Galvin (2016) and Esterhuizen (2007). Slenderness ratio (λ) is the term used in civil engineering to describe the relationship between the unsupported height of a column and its lateral dimension. It differentiates short columns from long columns (Fig. 4b). The design of short columns or pillars is controlled by column dimension and material strength whereas the design of slender columns is governed by the column slenderness. Hu et al. (2021) discussed the role of stress and slenderness in buckling failure resulting from columns from foliation in rockmasses.

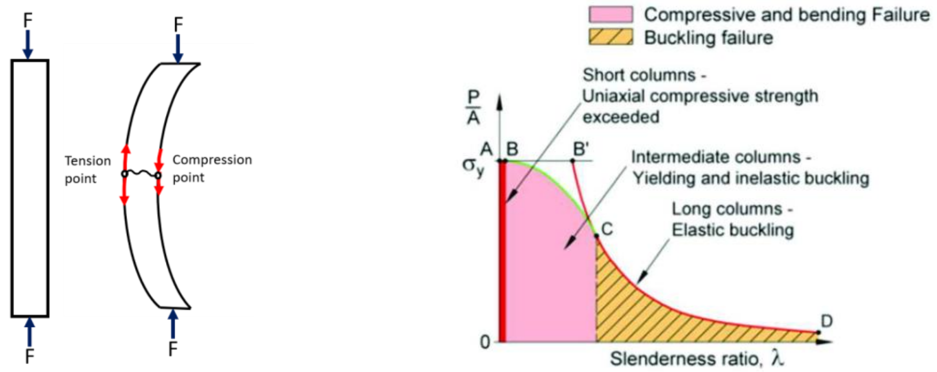

(a) Left: original state of column; Right: buckling of column on increased loading

(b) Classification of columns based on slenderness ratio (Gavin 2016)

Fig. 4 (a) Failure mechanism of tall pillars is buckling by bending and tension originating from outer fibre. (b) Slenderness ratio plot is recommended to consider for the design of tall pillars.

The study results may have implications for the design of underground pillars in rock. In current traditional pillar design the pillar strength equations are a function of the pillar intact rock damage initiation compressive strength and the pillar width to height ratio. For pillars with H/D≥6, consideration may be given to redefining the pillar strength as a function of its intact rock tensile strength.

4 Conclusions

When the stability of the walls of underground excavations and pillars are structurally controlled because of close spacing of vertical and or sub-horizontal discontinuities, the use of the intact rock compressive strength is inappropriate in the design of these underground structures. Numerical modelling and laboratory testing show that rock and concrete specimens with H/D ≥ 6 tend to fail in tension by bending rather than by tensile splitting, shear or crushing. The failure characteristics of these columns and beams suggest that the most vital parameter in the design is the tensile strength of their intact rock rather than their uniaxial compressive strength. Hence, the tensile strength of the rock should be used for strength estimations of tall pillars, columns, or beams with H/≥ 6.

This research is ongoing and is dedicated to finding practical and meaningful solutions to the critical design issues often ignored or overlooked, but which have crucial impact on mine safety and productivity.

ACKNOWLEDGEMENTS

This study is supported by Nazarbayev University Faculty Development Competitive Research Grant Program number 201223FD8835. We also acknowledge Kazzinc Kazakhstan-based Mining and Metallurgical Company for providing the rock specimens for this research.

References

Baizhiyen, N (2019) Design of tall underground mine pillars. MSc thesis at the School of Mining and Geosciences, Nazarbayev University, Astana.

Basu, A, Mishra, D. A, & Roychowdhury, K (2013) Rock failure modes under uniaxial compression, Brazilian, and point load tests. Bulletin of Engineering Geology and the environment, 72, 457-475.

Cai, M, Kaiser P.K (2018) Rockburst Support Reference Book Volume 1 Rockburst Phenomenon and Support Characteristics. MIRARCO, Laurentian University, Canada.

Esterhuizen, G.S, & Ellenberger, J.L (2007) Effects of weak bands on pillar stability in stone mines. Field observations and numerical model assessment. Proceedings of the 26th International Conference on Ground Control in Mining. Morgantown, 336–342. http://www.cdc.gov/niosh/mining/.

Esterhuizen, G.S (2006) Evaluation of the strength slender pillars. Transactions-society for Mining Metallurgy and Exploration Incorporated, 320, pp. 69-76.

Galvin, J.M (2016) Ground Engineering - Principles and Practices for Underground Coal Mining. ACARP: Springer.

Hawkins, A.B (1998) Aspects of rock strength. Bull. Eng. Geol. Environ. 1998; 57:17–30

Hoek E., Kaiser, P.K. and Bawden, W (1995) Support of underground excavations in hard rocks. Rotterdam.

Jia, P, and Tang, C. A (2008) Numerical study on failure mechanism of tunnel in jointed rock mass. Tunnelling and Underground Space Technology, *23*(5), 500-507.

Jin, C, Shao A, Liu, L, Han, T. Fan, F, Li, S (2018) Failure Mechanism of Highly Stressed Rock Mass during Unloading Based on the Stress Arch Theory. Int. J. Geomech., 2018, 18(11): 04018146.

Karampinos, E, Hadjigeorgiou, J, Hazzard, J, & Turcotte, P (2015) Discrete element modelling of the buckling phenomenon in deep hard rock mines. International Journal of Rock Mechanics and Mining Sciences, 80, 346-356.

Kong, X, Liu, Q, & Lu, H (2021) Effects of rock specimen size on mechanical properties in laboratory testing. Journal of Geotechnical and Geoenvironmental Engineering, 147(5), 04021013.

Krauland, N and Soder, P.E (1987) Determining pillar strength from pillar failure observation. Engineering and Mining Journal, vol. 8, pp. 34 – 40.23.

Lunder, P.J (1994) Hard rock pillar strength estimation: An applied empirical approach. MSc thesis, University of British Columbia, Vancouver, Cananda.

Mark, C, & Barton, T. M (1996) The uniaxial compressive strength of coal: should it be used to design pillars. In Proceedings of the 15th International Conference on Ground Control in Mining. Golden, CO: Colorado School of Mines (pp. 61-78).

Masoudi R, Sharifzadeh, M (2018) Reinforcement selection for deep and high-stress tunnels at preliminary design stages using ground demand and support capacity approach. International Journal of Mining Science and Technology 28 (2018) 573–582.

Masoumi, H, Douglas, K, Saydam, S, and Hagan, P (2012) Experimental study of size effects of rock on UCS and point load tests. Proc., 46th U.S. Rock Mechanics Geomechanics Symp., American Rock Mechanics Association, Chicago, 2561–2568.

Masoumi, H, Saydam, S, and Hagan, P. C (2015) Unified size-effect law for intact rock. Int. J. Geomech., 10.1061/(ASCE)GM.1943-5622.0000543, 04015059.

Masoumi, H, Roshan, H, Hedayat, A, & Hagan, P. C (2018) Scale-size dependency of intact rock under point-load and indirect tensile Brazilian testing. International Journal of Geomechanics, 18(3), 04018006. Popov, E.P. (1978). Mechanics of Materials. 2nd. Prentice Hall Inc.

RocScience 2019 RS2 Manual.

Sharrock G.B, Chapula, B (2020) Anisotropic rock mass behaviour in high-displacement ground at CSA mine. The Journal of the Southern African Institute of Mining and Metallurg. DOI ID: http://dx.doi.org/10.17159/2411 9717/863/2020

Ulusay, R (2015) The ISRM suggested methods for rock characterization, testing and monitoring: 2007-2014. Springer.

Vogler, U.W.O.L. and Stacey, T.R (2016) The influence of test specimen geometry on the laboratory-determined class II characteristics of rocks, J S. Afr. Inst. Min. Metall., Vol 116, No 11, November, pp 987-1000.2.

Zhou, J, Pan, J, Xia, Y, Du, T, Liu, W, & Zhang, C (2024) Mechanism and prevention of coal bursts in gob-side roadway floor under thick and hard roof in the deep mining area of Ordos. International Journal of Coal Science & Technology, 11(1), 80.